Analysis of a Fluid-Loaded Thick Plate

Andrew J. Hull
Submarine Sonar Department

NAVSEA

NEWPORT

Undersea Warfare Center Division

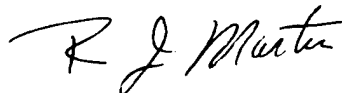# Naval Undersea Warfare Center Division Newport, Rhode Island

20030106 072

PREFACE

This report, prepared under Project No. R62300, was sponsored by the In-House Laboratory Independent Research (ILIR) Program.

The technical reviewer for this report was Anthony J. Kalinowski (Code 74).

The author wishes to thank Karen Holt (Code 543) for her help with the editing of the manuscript.

Reviewed and Approved: 1 October 2002

Ronald J. Martin
Head, Submarine Sonar Department

REPORT DOCUMENTATION PAGE

Form Approved
OMB No. 0704-0188

1. AGENCY USE ONLY *(Leave blank)*	2. REPORT DATE 1 October 2002	3. REPORT TYPE AND DATES COVERED

4. TITLE AND SUBTITLE

Analysis of a Fluid-Loaded Thick Plate

5. FUNDING NUMBERS

6. AUTHOR(S)

Andrew J. Hull

7. PERFORMING ORGANIZATION NAME(S) AND ADDRESS(ES)

Naval Undersea Warfare Center Division
1176 Howell Street
Newport, RI 02841-1708

8. PERFORMING ORGANIZATION REPORT NUMBER

TR 11,389

9. SPONSORING/MONITORING AGENCY NAME(S) AND ADDRESS(ES)

10. SPONSORING/MONITORING AGENCY REPORT NUMBER

11. SUPPLEMENTARY NOTES

12a. DISTRIBUTION/AVAILABILITY STATEMENT

Approved for public release; distribution is unlimited.

12b. DISTRIBUTION CODE

13. ABSTRACT (Maximum 200 words)

This report describes the closed-form expressions for insertion loss and echo reduction, which are derived using a thick plate model that is loaded with either one or two fluids at any acoustic wavenumber. The equations of motion for the plate are coupled to the acoustic wave equation at the plate boundaries, generating a four-by-four system of linear equations with dilatational and shear wave propagation coefficients as the unknown quantities. These unknowns are solved in closed form and inserted back into the displacement equations. Once the displacements are known, the reflected and transmitted pressure can be calculated, which results in the closed-form solution to insertion loss and echo reduction at all wavenumbers.

The solutions are then compared to previously available expressions for insertion loss and echo reduction with the incoming wave at normal incidence (zero wavenumber). Additionally, closed-form transfer functions of plate displacement divided by excitation and plate displacement on one side divided by plate displacement on the other side are derived for a thick plate with fluid loading on one or both sides. Based on these transfer functions, the displacement shape of the plate modes is formulated. It is shown that the plate with no fluid loading and the plate with single-sided fluid loading have the same displacement shape and that the plate with double fluid loading has a different displacement shape for each plate mode. The effects of the dispersion curves are also studied and discussed.

14. SUBJECT TERMS

Closed-Form Solutions	Fluid Loading	Reflected Energy	Thick Plate Theory
Echo Reduction	Insertion Loss	Thick Plate Modeling	Transmitted Energy

15. NUMBER OF PAGES
46

16. PRICE CODE

17. SECURITY CLASSIFICATION OF REPORT Unclassified	18. SECURITY CLASSIFICATION OF THIS PAGE Unclassified	19. SECURITY CLASSIFICATION OF ABSTRACT Unclassified	20. LIMITATION OF ABSTRACT SAR

TABLE OF CONTENTS

LIST OF ILLUSTRATIONS

LIST OF ILLUSTRATIONS (Cont'd)

ANALYSIS OF A FLUID-LOADED THICK PLATE

INTRODUCTION

The physics of a thick plate with fluid loading on both sides provides the theoretical basis for insertion loss and echo reduction tests, both of which are typically used to determine how efficiently a material transmits or reflects energy. Such testing is conducted by insonifying a submerged, slab-shaped sample and then measuring the transmitted and reflected sound pressure. Based on the sound pressure level of the incident field, the insertion loss and echo reduction quantities can be calculated. When these experiments are performed in a small tank, the wall motion of the sample is sometimes measured, with the fluid pressure then calculated based on this displacement. The above measurements and corresponding theory are important to the U.S. Navy because they help designers develop the most effective acoustic sonar windows, sonar and ship baffles, and anechoic marine coatings.

Central to the study and understanding of insertion loss and echo reduction is plate theory, which has been researched extensively for many years. Thin plate theory,[1] studied in 1973, is a simplified version that fails to accurately incorporate dynamic response when the sample is thick compared to a wavelength. In contrast, thick plate theory[2] usually incorporates all the dynamics of the plate and is normally used when the sample is on the order of a wavelength of energy in the structure. More complex investigations have analyzed the dispersion curve for the plate without fluid loading[3-5] or for the plate in contact with a continuous fluid on one or both sides.[6-11] To a lesser extent, papers have been published that examine plate response to various other loading configurations. For example, studies have explored the radiation efficiency of infinite fluid-loaded plates subjected to point loads,[12] calculated the corresponding transfer functions for thin plate models coupled to fluid loading,[13] and determined mode shapes for a thick plate with finite depth that is loaded by fluid on both sides.[14] During these investigations, the response of thick-walled plates has been typically left as an open-form solution that involves a matrix inverse at a specific wavenumber and frequency. Although closed-form solutions have been previously derived, such analyses have been performed only at zero wavenumbers and have not been extended to nonzero wavenumbers.

1

This report derives the equations of motion of an infinite thick plate coupled on one or both sides with fluid loading as it is excited with a continuous forcing function. The equations of motion are formulated into a four-by-four system of linear equations with wave propagation coefficients as the unknown terms. Once the system matrix is known, the dispersion equations — derived in closed-form expressions from the determinant of the matrix — explicitly show the effects of the fluid loading. Calculated next are the closed-form transfer functions of plate motion divided by source excitation, which contain the plate and the fluid terms separately. Based on these transfer functions, the displacement shape of the plate modes is studied with respect to fluid loading on one or both sides of the plate. Insertion loss and echo reduction are then calculated for the system at nonzero wavenumbers using closed-form solutions of the pressure fields that are determined based on plate wall motion, with these results compared to the previously available values at zero wavenumber.

SYSTEM MODEL

As shown in figures 1 and 2, the system model is a thick plate in contact on one or both sides with a fluid that exerts a continuous excitation pressure on the plate. The model configurations, referred to as single and double fluid-loaded plates, are based on the following assumptions: (1) the forcing function acting on the plate is a plane wave with definite wavenumber and frequency content, (2) the corresponding response of the plate is at a definite wavenumber and frequency, (3) motion is normal and tangential to the plate in one direction (two-dimensional system), (4) the plate has an infinite spatial extent, (5) the particle motion and pressure response is linear, and (6) the fluid medium has no loss. For the case where the fluid is on both sides of the plate, each fluid has the same acoustic properties.

For the single and double fluid-loaded plates, the acoustic pressure in the fluid on the excitation side of the plate is governed by the wave equation and is written in Cartesian coordinates as[15]

$$\frac{\partial^2 p_1(x,z,t)}{\partial z^2} + \frac{\partial^2 p_1(x,z,t)}{\partial x^2} - \frac{1}{c_f^2}\frac{\partial^2 p_1(x,z,t)}{\partial t^2} = 0 \,, \tag{1}$$

2
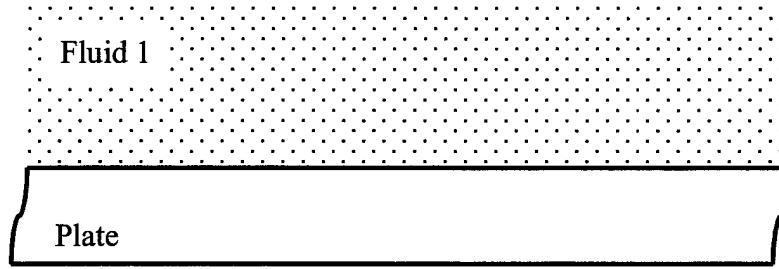
Figure 1. Single Fluid-Loaded Plate

Figure 2. Double Fluid-Loaded Plate

where $p_1(x,z,t)$ is the pressure (N/m^2), with the subscript 1 denoting the fluid on the excitation side of the plate; z is the spatial location (m) normal to the plate; x is the spatial location (m) tangential to the plate; c_f is the compressional wave speed of the fluid (m/s); and t is time (s). The coordinate system of this configuration is shown in figure 3. Note that the use of this orientation results in $b = 0$ and a having a value less than zero. Furthermore, the thickness of the plate, h, is a positive value, and the motion of the plate is governed by the equation[16]

$$\mu\nabla^2\mathbf{u} + (\lambda + \mu)\nabla\nabla \bullet \mathbf{u} = \rho\frac{\partial^2\mathbf{u}}{\partial t^2} ,\tag{2}$$

where ρ is the density (kg/m^3), λ and μ are the Lamé constants (N/m^2), $\bullet$ denotes a vector dot product, and $\mathbf{u}$ is the Cartesian coordinate displacement vector of the plate. For the double

3
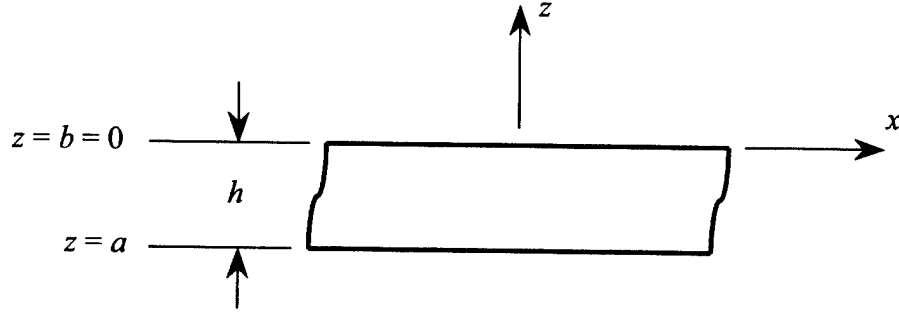
Figure 3. Coordinate System of Model

fluid-loaded plate, the acoustic pressure in the fluid opposite the excitation side of the plate is governed by the wave equation and is written in Cartesian coordinates as

$$\frac{\partial^2 p_2(x,z,t)}{\partial z^2} + \frac{\partial^2 p_2(x,z,t)}{\partial x^2} - \frac{1}{c_f^2}\frac{\partial^2 p_2(x,z,t)}{\partial t^2} = 0 \ , \tag{3}$$

where $p_2(x,z,t)$ is the pressure (N/m^2) and the subscript 2 denotes the fluid opposite the excitation side of the plate. For the single and double fluid-loaded plates, the interface between the first fluid and the surface of the plate at $z = b$ satisfies the linear momentum equation, which is[17]

$$\rho_f \frac{\partial^2 u_z(x,b,t)}{\partial t^2} = -\frac{\partial p_1(x,b,t)}{\partial z} \ , \tag{4}$$

where ρ_f is the density of the fluid (kg/m^3). For the double fluid-loaded plate, the interface between the second fluid and the surface of the plate at $z = a$ also satisfies the linear momentum equation and is written as

$$\rho_f \frac{\partial^2 u_z(x,a,t)}{\partial t^2} = -\frac{\partial p_2(x,a,t)}{\partial z} \ . \tag{5}$$

Equations (1) through (5) are the governing partial differential equations of the single and double fluid-loaded plate systems.

4

Equations (1) through (3) are now transformed from partial differential equations into ordinary differential equations and then into algebraic expressions. The acoustic pressure in equation (1) is modeled as a function at definite wavenumber and frequency by

$$p_1(x,z,t) = P_1(z,k_x,\omega)\exp(ik_x x)\exp(i\omega t) \ , \tag{6}$$

where ω is frequency (rad/s), k_x is the spatial wavenumber in the x-direction (rad/m), and i is the square root of -1. If the pressure in the fluid is generated by an acoustic plane wave, the spatial wavenumber is given by

$$k_x = \frac{\omega}{c_f}\sin(\theta) \ , \tag{7}$$

where θ is the angle of incidence (rad) of the incoming acoustic wave, with $\theta = 0$ corresponding to excitation normal to the plate (or broadside excitation). Wavenumbers larger than ω/c_f are possible and are typically generated from turbulent fluid loading or structural wave loading. Inserting equation (6) into equation (1) and solving the resulting ordinary differential equation yields

$$P_1(z,k_x,\omega) = H(k_x,\omega)\exp(i\gamma z) + P_e(\omega)\exp(-i\gamma z) \ . \tag{8}$$

In equation (8), the first term on the right-hand side represents the reflected (or reradiated) pressure field and the second term represents the applied incident pressure field (the excitation or forcing function) acting on the plate. To be exact, the term $H(k_x,\omega)$ is the wave propagation coefficient of the reflected pressure field, and the term $P_e(\omega)$ is the excitation (or source) level. Furthermore,

$$\gamma = \sqrt{\left(\frac{\omega}{c_f}\right)^2 - k_x^2} \ , \tag{9}$$

where γ is the wavenumber of the acoustic pressure in the fluid (rad/m).

Equation (2) is manipulated by writing the Cartesian coordinate displacement vector **u** as

$$\mathbf{u} = \begin{Bmatrix} u_x(x,y,z,t) \\ u_y(x,y,z,t) \\ u_z(x,y,z,t) \end{Bmatrix} , \tag{10}$$

with y denoting the direction into the plate. The symbol ∇, from equation (2), is the gradient vector differential operator written in three-dimensional Cartesian coordinates as[18]

$$\nabla = \frac{\partial}{\partial x} i_x + \frac{\partial}{\partial y} i_y + \frac{\partial}{\partial z} i_z , \tag{11}$$

with i_x denoting the unit vector in the x-direction, i_y denoting the unit vector in the y-direction, and i_z denoting the unit vector in the z-direction. The symbol ∇^2 is the three-dimensional Laplace operator operating on vector **u** as

$$\nabla^2 \mathbf{u} = \nabla^2 u_x i_x + \nabla^2 u_y i_y + \nabla^2 u_z i_z \tag{12}$$

and on scalar u as

$$\nabla^2 u_{x,y,z} = \nabla \bullet \nabla u_{x,y,z} = \frac{\partial^2 u_{x,y,z}}{\partial x^2} + \frac{\partial^2 u_{x,y,z}}{\partial y^2} + \frac{\partial^2 u_{x,y,z}}{\partial z^2} ; \tag{13}$$

the term $\nabla \bullet \mathbf{u}$ is the divergence, which is equal to

$$\nabla \bullet \mathbf{u} = \frac{\partial u_x}{\partial x} + \frac{\partial u_y}{\partial y} + \frac{\partial u_z}{\partial z} . \tag{14}$$

The displacement vector **u** is written as

$$\mathbf{u} = \nabla \phi + \nabla \times \bar{\psi} , \tag{15}$$

where ϕ is a dilatational scalar potential, $\times$ denotes a vector crossproduct, and $\bar{\psi}$ is an equivoluminal vector potential expressed as

6

$$\vec{\psi} = \begin{Bmatrix} \psi_x(x,y,z,t) \\ \psi_y(x,y,z,t) \\ \psi_z(x,y,z,t) \end{Bmatrix} . \tag{16}$$

The formulation is a two-dimensional problem; thus, $y \equiv 0$ and $\partial(\cdot)/\partial y \equiv 0$. Expanding equation (15) and breaking the displacement vector into its individual nonzero terms yields

$$u_x(x,z,t) = \frac{\partial \phi(x,z,t)}{\partial x} - \frac{\partial \psi_y(x,z,t)}{\partial z} \tag{17}$$

and

$$u_z(x,z,t) = \frac{\partial \phi(x,z,t)}{\partial z} + \frac{\partial \psi_y(x,z,t)}{\partial x} . \tag{18}$$

Equations (17) and (18) are next inserted into equation (2), which results in

$$c_d^2 \nabla^2 \phi(x,z,t) = \frac{\partial^2 \phi(x,z,t)}{\partial t^2} \tag{19}$$

and

$$c_s^2 \nabla^2 \psi_y(x,z,t) = \frac{\partial^2 \psi_y(x,z,t)}{\partial t^2} , \tag{20}$$

where equation (19) corresponds to the dilatational component and equation (20) corresponds to the shear component of the displacement field.[19] Correspondingly, the constants c_d and c_s are the complex dilatational and shear wave speeds, respectively, and are determined by

$$c_d = \sqrt{\frac{\lambda + 2\mu}{\rho}} \tag{21}$$

and

$$c_s = \sqrt{\frac{\mu}{\rho}} . \tag{22}$$

The relationships of the Lamé constants to the Young's (compressional) and shear moduli are shown as

$$\lambda = \frac{E\upsilon}{(1+\upsilon)(1-2\upsilon)} \tag{23}$$

and

$$\mu = G = \frac{E}{2(1+\upsilon)} \ , \tag{24}$$

where E is the Young's modulus (N/m^2), G is the shear modulus (N/m^2), and υ is the Poisson's ratio of the material (dimensionless).

The conditions of infinite length and steady-state response are now imposed, allowing the scalar and vector potential to be written as

$$\phi(x,z,t) = \Phi(z)\exp(ik_x x)\exp(i\omega t) \tag{25}$$

and

$$\psi_y(x,z,t) = \Psi(z)\exp(ik_x x)\exp(i\omega t) \ . \tag{26}$$

Inserting equation (25) into equation (19) yields

$$\frac{d^2\Phi(z)}{dz^2} + \alpha^2\Phi(z) = 0 \ , \tag{27}$$

where

$$\alpha = \sqrt{k_d^2 - k_x^2} \ , \tag{28}$$

with

$$k_d = \frac{\omega}{c_d} \ . \tag{29}$$

Inserting equation (26) into equation (20) produces

8

$$\frac{d^2\Psi(z)}{dz^2} + \beta^2\Psi(z) = 0 \ , \tag{30}$$

where

$$\beta = \sqrt{k_s^2 - k_x^2} \ , \tag{31}$$

with

$$k_s = \frac{\omega}{c_s} \ . \tag{32}$$

The solution to equation (27) is

$$\Phi(z) = A(k_x,\omega)\exp(i\alpha z) + B(k_x,\omega)\exp(-i\alpha z) \ , \tag{33}$$

and the solution to equation (30) is

$$\Psi(z) = C(k_x,\omega)\exp(i\beta z) + D(k_x,\omega)\exp(-i\beta z) \ , \tag{34}$$

where $A(k_x,\omega)$, $B(k_x,\omega)$, $C(k_x,\omega)$, and $D(k_x,\omega)$ are wave propagation constants of the plate and are determined below. The displacements, now written as functions of the unknown constants using the expressions in equations (17) and (18), are

$$u_x(x,z,t) = U_x(k_x,z,\omega)\exp(ik_x x)\exp(i\omega t)$$

$$\begin{aligned} = \big[&A(k_x,\omega)ik_x \exp(i\alpha z) + B(k_x,\omega)ik_x \exp(-i\alpha z) \\ &- C(k_x,\omega)i\beta \exp(i\beta z) + D(k_x,\omega)i\beta \exp(-i\beta z) \big]\exp(ik_x x)\exp(i\omega t) \end{aligned} \tag{35}$$

and

$$u_z(x,z,t) = U_z(k_x,z,\omega)\exp(ik_x x)\exp(i\omega t)$$

$$\begin{aligned} = \big[&A(k_x,\omega)i\alpha \exp(i\alpha z) - B(k_x,\omega)i\alpha \exp(-i\alpha z) \\ &+ C(k_x,\omega)ik_x \exp(i\beta z) + D(k_x,\omega)ik_x \exp(-i\beta z) \big]\exp(ik_x x)\exp(i\omega t) . \end{aligned} \tag{36}$$

9

The normal stress at the top of the plate ($z = b$) is equal to the opposite of the pressure in the fluid and is expressed as

$$\tau_{zz}(x,b,t) = (\lambda + 2\mu)\frac{\partial u_z(x,b,t)}{\partial z} + \lambda\frac{\partial u_x(x,b,t)}{\partial x} = -p_1(x,b,t) \ . \tag{37}$$

The tangential stress at the top of the plate is zero and is written as

$$\tau_{zx}(x,b,t) = \mu\left[\frac{\partial u_x(x,b,t)}{\partial z} + \frac{\partial u_z(x,b,t)}{\partial x}\right] = 0 \ . \tag{38}$$

For the double fluid-loaded plate, the normal stress at the bottom of the plate ($z = a$) is equal to the opposite of the pressure in the fluid. This expression is

$$\tau_{zz}(x,a,t) = (\lambda + 2\mu)\frac{\partial u_z(x,a,t)}{\partial z} + \lambda\frac{\partial u_x(x,a,t)}{\partial x} = -p_2(x,a,t) \ , \tag{39}$$

where $p_2(x,a,t)$ represents the transmitted (or radiated) acoustic pressure in the fluid field on the opposite side of the acoustic excitation. For the single fluid-loaded plate, $p_2(x,z,t) \equiv 0$ in equation (39). The tangential stress at the bottom of the plate is zero, with this equation written as

$$\tau_{zx}(x,a,t) = \mu\left[\frac{\partial u_x(x,a,t)}{\partial z} + \frac{\partial u_z(x,a,t)}{\partial x}\right] = 0 \ . \tag{40}$$

For the double fluid-loaded plate, the acoustic pressure in equation (3) is modeled as a function at definite wavenumber and frequency, resulting in

$$p_2(x,z,t) = P_2(z,k_x,\omega)\exp(ik_x x)\exp(i\omega t) \ . \tag{41}$$

Inserting equation (41) into equation (3) and solving the resulting ordinary differential equation yields

$$P_2(z,k_x,\omega) = K(k_x,\omega)\exp(-i\gamma z) \ , \tag{42}$$

10

which is the transmitted (or outgoing) acoustic energy in the second fluid. The term $K(k_x, \omega)$ is the wave propagation coefficient of the transmitted pressure field. Note that there is no incoming wave energy on this side of the plate and thus only one exponential term is present.

Assembling equations (37) through (40); incorporating equations (4), (5), (8), and (42); and letting $b = 0$ yields the four-by-four system of linear equations that model the system as follows:

$$\mathbf{Ax = b} \, , \tag{43}$$

where the entries of equation (43) are

$$A_{11p} = -\alpha^2 \lambda - 2\alpha^2 \mu - \lambda k_x^2 \, , \tag{44}$$

$$A_{11s} = A_{11d} = \frac{\rho_f \omega^2 \alpha}{\gamma} \, , \tag{45}$$

$$A_{11} = A_{11p} + A_{11s} \, , \tag{46}$$

$$A_{12} = A_{11p} - A_{11s} \, , \tag{47}$$

$$A_{13p} = 2k_x \beta \mu \, , \tag{48}$$

$$A_{13s} = A_{13d} = \frac{\rho_f \omega^2 k_x}{\gamma} \, , \tag{49}$$

$$A_{13} = -A_{13p} + A_{13s} \, , \tag{50}$$

$$A_{14} = A_{13p} + A_{13s} \, , \tag{51}$$

$$A_{21} = -2\mu k_x \alpha \, , \tag{52}$$

$$A_{22} = -A_{21} \, , \tag{53}$$

$$A_{23} = \mu \beta^2 - \mu k_x^2 \, , \tag{54}$$

$$A_{24} = A_{23} \, , \tag{55}$$

$$A_{31} = \left(A_{11p} - A_{11d}\right)\exp(\mathrm{i}\alpha a) \ , \tag{56}$$

$$A_{32} = \left(A_{11p} + A_{11d}\right)\exp(-\mathrm{i}\alpha a) \ , \tag{57}$$

$$A_{33} = \left(-A_{13p} - A_{13d}\right)\exp(\mathrm{i}\beta a) \ , \tag{58}$$

$$A_{34} = \left(A_{13p} - A_{13d}\right)\exp(-\mathrm{i}\beta a) \ , \tag{59}$$

$$A_{41} = A_{21}\exp(\mathrm{i}\alpha a) \ , \tag{60}$$

$$A_{42} = -A_{21}\exp(-\mathrm{i}\alpha a) \ , \tag{61}$$

$$A_{43} = A_{23}\exp(\mathrm{i}\beta a) \ , \tag{62}$$

$$A_{44} = A_{23}\exp(-\mathrm{i}\beta a) \ , \tag{63}$$

$$x_{11} = A(k_x,\omega) \ , \tag{64}$$

$$x_{21} = B(k_x,\omega) \ , \tag{65}$$

$$x_{31} = C(k_x,\omega) \ , \tag{66}$$

$$x_{41} = D(k_x,\omega) \ , \tag{67}$$

$$b_{11p} = -P_e(\omega) \ , \tag{68}$$

$$b_{11s} = -P_e(\omega) \ , \tag{69}$$

$$b_{11} = b_{11p} + b_{11s} \ , \tag{70}$$

$$b_{21} = 0 \ , \tag{71}$$

$$b_{31} = 0 \ , \tag{72}$$

and

$$b_{41} = 0 \ . \tag{73}$$

In equations (44) through (73), the subscript p corresponds to terms related to the plate, the subscript s corresponds to the case of both the single and double fluid-loaded plates, and the

12

subscript d corresponds only to the case of the double fluid-loaded plate. To model the behavior of the thick plate without the fluid loads, the terms with the subscript s and d are set equal to zero. To model the behavior of the fluid plate with a single fluid load, the terms with the subscript d are set equal to zero.

For the single and double fluid-loaded plate, the reflected acoustic field on the excitation side of the plate is

$$P_R(k_x, z_b, \omega) = \left[\left(\frac{\omega^2 \rho_f}{i\gamma} \right) U_z(k_x, b, \omega) + 1 \right] \exp(i\gamma z_b) , \qquad (74)$$

with z_b being the position where the field is evaluated (m). The total pressure field on the excitation side is a sum of the reflected field and the spatially phase-shifted excitation level. It is written as

$$P_{Total}(k_x, z_b, \omega) = P_R(k_x, z_b, \omega) + P_e(\omega) \exp(-i\gamma z_b) . \qquad (75)$$

For the double fluid-loaded plate, the transmitted pressure field on the opposite side of the excitation is

$$P_T(k_x, z_a, \omega) = \left[\left(\frac{-\omega^2 \rho_f}{i\gamma} \right) U_z(k_x, a, \omega) \right] \exp(-i\gamma z_a) , \qquad (76)$$

with z_a being the position where the field is evaluated (m). The insertion loss (IL) of the double fluid-loaded plate is then calculated using[20]

$$IL(k_x, \omega) = 20 \log_{10} \left| \frac{P_e(\omega)}{P_T(k_x, \omega)} \right| , \qquad (77)$$

where $IL(k_x, \omega)$ is in units of decibels. The echo reduction (ER) is calculated using[20]

13

$$ER(k_x,\omega) = 20\log_{10}\left|\frac{P_e(\omega)}{P_R(k_x,\omega)}\right| , \qquad (78)$$

where $ER(k_x,\omega)$ is in units of decibels.

DISPERSION EQUATIONS

The dispersion equation is an equation whose zeros correspond to single-mode propagation in the structure. This function is proportional to the determinant of **A** in equation (43). For the case of the single fluid-loaded plate, the equation is written as

$$\begin{aligned}
\Delta_s(k_x,\omega) = {} & p_1(k_x,\omega)\cos(\alpha h)\cos(\beta h) + f_1(k_x,\omega)\cos(\alpha h)\sin(\beta h) \\
& + f_2(k_x,\omega)\sin(\alpha h)\cos(\beta h) + p_2(k_x,\omega)\sin(\alpha h)\sin(\beta h) - p_1(k_x,\omega) ,
\end{aligned} \qquad (79)$$

where

$$p_1(k_x,\omega) = -8\alpha\beta k_x^2(\beta^2 - k_x^2)^2 , \qquad (80)$$

$$f_1(k_x,\omega) = i\rho_f(\gamma\rho)^{-1}\alpha(\beta^2 - k_x^2)^2(\beta^2 + k_x^2)^2 , \qquad (81)$$

$$f_2(k_x,\omega) = 4i\rho_f(\gamma\rho)^{-1}\alpha^2\beta k_x^2(\beta^2 + k_x^2)^2 , \qquad (82)$$

and

$$p_2(k_x,\omega) = (\beta^2 - k_x^2)^4 + 16\alpha^2\beta^2 k_x^4 . \qquad (83)$$

For the case of the double fluid-loaded plate, the equation is written as

$$\begin{aligned}
\Delta_d(k_x,\omega) = {} & p_1(k_x,\omega)\cos(\alpha h)\cos(\beta h) + 2f_1(k_x,\omega)\cos(\alpha h)\sin(\beta h) \\
& + 2f_2(k_x,\omega)\sin(\alpha h)\cos(\beta h) \\
& + \left[p_2(k_x,\omega) + f_3(k_x,\omega)\right]\sin(\alpha h)\sin(\beta h) - p_1(k_x,\omega) ,
\end{aligned} \qquad (84)$$

14

where

$$f_3(k_x, \omega) = \rho_f^2 (\gamma \rho)^{-2} \alpha^2 (\beta^2 + k_x^2)^4 \ . \tag{85}$$

In equations (79) and (84), the p constants correspond to the plate and the f constants correspond to the fluid loads. In the absence of fluid loading, the f constants are identically zero.

It is noted that these dispersion curves without the fluid load and with the double fluid load have both been previously derived. The plate dispersion curve without fluid loading is known as the Rayleigh-Lamb frequency equation for the propagation of waves in a plate, which is given as[19]

$$\frac{\tan(\beta h/2)}{\tan(\alpha h/2)} + \left[\frac{4\alpha\beta k_x^2}{(k_x^2 - \beta^2)^2} \right]^{\pm 1} = 0 \ . \tag{86}$$

Equation (79) (or equation (84)) with $f_n = 0$ and equation (86), although not identical, have the same zeros that correspond to the branches of the dispersion curves for the plate without fluid loading. The plate dispersion curve with the double fluid load for the case of symmetrical wave response[6] is

$$4\left(1 - \frac{1}{2}\frac{c_p^2}{c_s^2}\right)^2 \coth\left[k_x \frac{h}{2}\left(1 - \frac{c_p^2}{c_d^2}\right)^{1/2}\right]$$

$$-4\left(1 - \frac{c_p^2}{c_d^2}\right)^{1/2}\left(1 - \frac{c_p^2}{c_s^2}\right)^{1/2} \coth\left[k_x \frac{h}{2}\left(1 - \frac{c_p^2}{c_s^2}\right)^{1/2}\right]$$

$$+ \frac{\rho_f c_f^2}{\rho c_s^2}\left(1 - \frac{c_p^2}{c_f^2}\right)^{-1/2} \frac{c_p^4}{c_f^2 c_s^2}\left(1 - \frac{c_p^2}{c_d^2}\right)^{1/2} = 0 \ , \tag{87}$$

and for the case of antisymmetrical response[6] is

15

$$4\left(1-\frac{1}{2}\frac{c_p^2}{c_s^2}\right)^2 \tanh\left[k_x \frac{h}{2}\left(1-\frac{c_p^2}{c_d^2}\right)^{1/2}\right]$$

$$-4\left(1-\frac{c_p^2}{c_d^2}\right)^{1/2}\left(1-\frac{c_p^2}{c_s^2}\right)^{1/2}\tanh\left[k_x\frac{h}{2}\left(1-\frac{c_p^2}{c_s^2}\right)^{1/2}\right]$$

$$+\frac{\rho_f c_f^2}{\rho c_s^2}\left(1-\frac{c_p^2}{c_f^2}\right)^{-1/2}\frac{c_p^4}{c_f^2 c_s^2}\left(1-\frac{c_p^2}{c_d^2}\right)^{1/2}=0 \ , \tag{88}$$

where

$$c_p = \frac{\omega}{k_x} \ . \tag{89}$$

Equation (84) and equations (87) and (88), although not identical, have the same zeros that correspond to the branches of the dispersion curves for the double fluid-loaded plate. Figures of calculated dispersion curves are shown in the numerical example section.

CLOSED-FORM TRANSFER FUNCTIONS

The closed-form transfer functions can be determined by solving equation (43) as

$$\mathbf{x} = \mathbf{A}^{-1}\mathbf{b} \ , \tag{90}$$

then taking the entries of $\mathbf{x}$ and inserting them into equations (35) and (36), and finally reducing the resultant expressions. For the single fluid-loaded plate, the transfer function of the tangential displacement at location z divided by the excitation level is equal to

$$\frac{U_x^s(k_x,z,\omega)}{P_e(\omega)} = \frac{U_x^{Ts}(k_x,z,\omega)}{\mu\Delta_s(k_x,\omega)} \ , \tag{91}$$

where

16

$$U_x^{Ts}(k_x, z, \omega) = p_3 \{\cos(\alpha z) - \cos(\beta h)\cos[\alpha(z+h)]\}$$
$$+ p_4 \{\cos(\beta z) - \cos(\alpha h)\cos[\beta(z+h)]\}$$
$$+ p_5 \sin(\alpha h)\sin[\beta(z+h)] + p_6 \sin(\beta h)\sin[\alpha(z+h)] , \qquad (92)$$

with

$$p_3(k_x, \omega) = 8i\alpha\beta k_x^3(\beta^2 - k_x^2) , \qquad (93)$$

$$p_4(k_x, \omega) = -4i\alpha\beta k_x(\beta^2 - k_x^2)^2 , \qquad (94)$$

$$p_5(k_x, \omega) = -16i\alpha^2\beta^2 k_x^3 , \qquad (95)$$

and

$$p_6(k_x, \omega) = 2ik_x(\beta^2 - k_x^2)^3 . \qquad (96)$$

For the single fluid-loaded plate, the transfer function of the normal displacement at location z divided by the excitation level is equal to

$$\frac{U_z^s(k_x, z, \omega)}{P_e(\omega)} = \frac{U_z^{Ts}(k_x, z, \omega)}{\mu\Delta_s(k_x, \omega)} , \qquad (97)$$

where

$$U_z^{Ts}(k_x, z, \omega) = p_7 \{\sin(\alpha z) - \cos(\beta h)\sin[\alpha(z+h)]\}$$
$$+ p_8 \{\sin(\beta z) - \cos(\alpha h)\sin[\beta(z+h)]\}$$
$$+ p_9 \sin(\alpha h)\cos[\beta(z+h)] + p_{10} \sin(\beta h)\cos[\alpha(z+h)] , \qquad (98)$$

with

$$p_7(k_x, \omega) = -8\alpha^2\beta k_x^2(\beta^2 - k_x^2) , \qquad (99)$$

$$p_8(k_x, \omega) = -4\alpha k_x^2(\beta^2 - k_x^2)^2 , \qquad (100)$$

$$p_9(k_x, \omega) = 16\alpha^2\beta k_x^4 , \qquad (101)$$

and

$$p_{10}(k_x, \omega) = 2\alpha(\beta^2 - k_x^2)^3 . \qquad (102)$$

17

The transfer function for the case of no fluid loading is given in equations (91) and (97), with the f terms set equal to zero and each equation divided by two.

For the double fluid-loaded plate, the transfer function of the tangential displacement at location z divided by the excitation level is equal to

$$\frac{U_x^d(k_x,z,\omega)}{P_e(\omega)} = \frac{U_x^{Td}(k_x,z,\omega)}{\mu\Delta_d(k_x,\omega)} \, ,$$ (103)

where

$$\begin{aligned}
U_x^{Td}(k_x,z,\omega) = &\ p_3\{\cos(\alpha z) - \cos(\beta h)\cos[\alpha(z+h)]\} \\
&+ p_4\{\cos(\beta z) - \cos(\alpha h)\cos[\beta(z+h)]\} \\
&+ p_5\sin(\alpha h)\sin[\beta(z+h)] + p_6\sin(\beta h)\sin[\alpha(z+h)] \\
&+ f_4\sin(\alpha h)\cos[\beta(z+h)] + f_5\sin(\beta h)\cos[\alpha(z+h)] \, ,
\end{aligned}$$ (104)

with

$$f_4(k_x,\omega) = 4\rho_f(\gamma\rho)^{-1}\alpha^2\beta k_x(\beta^2 + k_x^2)^2$$ (105)

and

$$f_5(k_x,\omega) = -2\rho_f(\gamma\rho)^{-1}\alpha k_x(\beta^2 - k_x^2)(\beta^2 + k_x^2)^2 \, .$$ (106)

For the double fluid-loaded plate, the transfer function of the normal displacement at location z divided by the excitation level is equal to

$$\frac{U_z^d(k_x,z,\omega)}{P_e(\omega)} = \frac{U_z^{Td}(k_x,z,\omega)}{\mu\Delta_d(k_x,\omega)} \, ,$$ (107)

where

$$\begin{aligned}
U_z^{Td}(k_x,z,\omega) = &\ p_7\{\sin(\alpha z) - \cos(\beta h)\sin[\alpha(z+h)]\} \\
&+ p_8\{\sin(\beta z) - \cos(\alpha h)\sin[\beta(z+h)]\} \\
&+ p_9\sin(\alpha h)\cos[\beta(z+h)] + p_{10}\sin(\beta h)\cos[\alpha(z+h)] \\
&+ f_6\sin(\alpha h)\sin[\beta(z+h)] + f_7\sin(\beta h)\sin[\alpha(z+h)] \, ,
\end{aligned}$$ (108)

with

$$f_6(k_x,\omega) = -4\mathrm{i}\rho_f(\gamma\rho)^{-1}\alpha^2 k_x^2(\beta^2 + k_x^2)^2$$ (109)

18

and

$$f_7(k_x,\omega) = -2i\rho_f(\gamma\rho)^{-1}\alpha^2(\beta^2 - k_x^2)(\beta^2 + k_x^2)^2 \ . \tag{110}$$

Several specific transfer functions of this system with a further reduced form are listed in the appendix. These functions correspond to displacement on one side of the plate divided by the displacement on the other side. Figures that compare the transfer functions are shown in the next section — A Numerical Example.

Once the closed-form transfer functions are known, closed-form expressions for the insertion loss and echo reduction can be determined by inserting equation (108) into equation (77) for insertion loss and into equation (78) for echo reduction. For the insertion loss term, this process results in

$$IL(k_x,\omega) = 20\log_{10}\left|\frac{-i\gamma\rho\Delta_d(k_x,\omega)}{\phi_I(k_x,\omega)}\right| \ , \tag{111}$$

where

$$\phi_I(k_x,\omega) = p_{11}(k_x,\omega)\sin(\alpha h) + p_{12}(k_x,\omega)\sin(\beta h) \ , \tag{112}$$

with

$$p_{11}(k_x,\omega) = 8\rho_f\alpha^2\beta k_x^2(\beta^2 + k_x^2)^2 \tag{113}$$

and

$$p_{12}(k_x,\omega) = 2\rho_f\alpha(\beta^2 - k_x^2)^2(\beta^2 + k_x^2)^2 \ . \tag{114}$$

For the echo reduction term, this process yields the expression

$$ER(k_x,\omega) = 20\log_{10}\left|\frac{\Delta_d(k_x,\omega)}{\phi_E(k_x,\omega)}\right| \ , \tag{115}$$

where

$$\phi_E(k_x,\omega) = p_1(k_x,\omega)\cos(\alpha h)\cos(\beta h) \\ + [p_2(k_x,\omega) - f_3(k_x,\omega)]\sin(\alpha h)\sin(\beta h) - p_1(k_x,\omega) \ . \tag{116}$$

19

A NUMERICAL EXAMPLE

A numerical example is discussed to illustrate the effects of fluid loading on a plate. A baseline problem is defined that corresponds to a mildly stiff elastomeric solid in contact with sea water on one or two sides. The plate material properties are as follows: Young's modulus is $E = 10^8$ N/m^2, density is $\rho = 1200$ kg/m^3, Poisson's ratio is $\upsilon = 0.4$ (dimensionless), and thickness is $h = 0.1$ m. The sea water has a compressional wave speed of $c_f = 1500$ m/s and a density of $\rho_f = 1025$ kg/m^3. The calculated Lamé constants are $\lambda = 1.43 \times 10^8$ N/m^2 and $\mu = 3.57 \times 10^7$ N/m^2. The calculated dilatational wave speed is $c_d = 423$ m/s, and the calculated shear wave speed is $c_s = 173$ m/s.

Figure 4 compares the dispersion curve (equation (79)) of the plate with a single fluid load (solid line) to the dispersion curve of a plate without fluid loading (dashed line). In figure 4 and the ensuing figures, the abscissa and ordinate have been normalized such that

$$\Omega = \frac{h\omega}{\pi c_s} \tag{117}$$

and

$$\kappa = \frac{hk}{\pi} , \tag{118}$$

where Ω is nondimensional frequency and κ is nondimensional wavenumber.

Figure 5 compares the dispersion curve (equation (84)) of the plate with a double fluid load (solid line) to the dispersion curve of a plate without fluid loading (dashed line). In general, most of the waves tend to be slowed down by the addition of either a single or double fluid load. In this figure, the solid line originating at the origin and terminating at approximately $\Omega = 10$ and $\kappa = 1.15$ corresponds to a compressional wave in the fluid,[*] which corresponds to transfer function nulls rather than maximum response.

The dispersion curves shown in figures 4 and 5 are useful for a number of reasons. Specifically, they relate frequency to the wavenumber of propagating waves in an unbounded

---

[*]In figure 4, this compressional wave is represented by the nearly vertical broken line in the first and second grids on the left-hand side of the illustration.
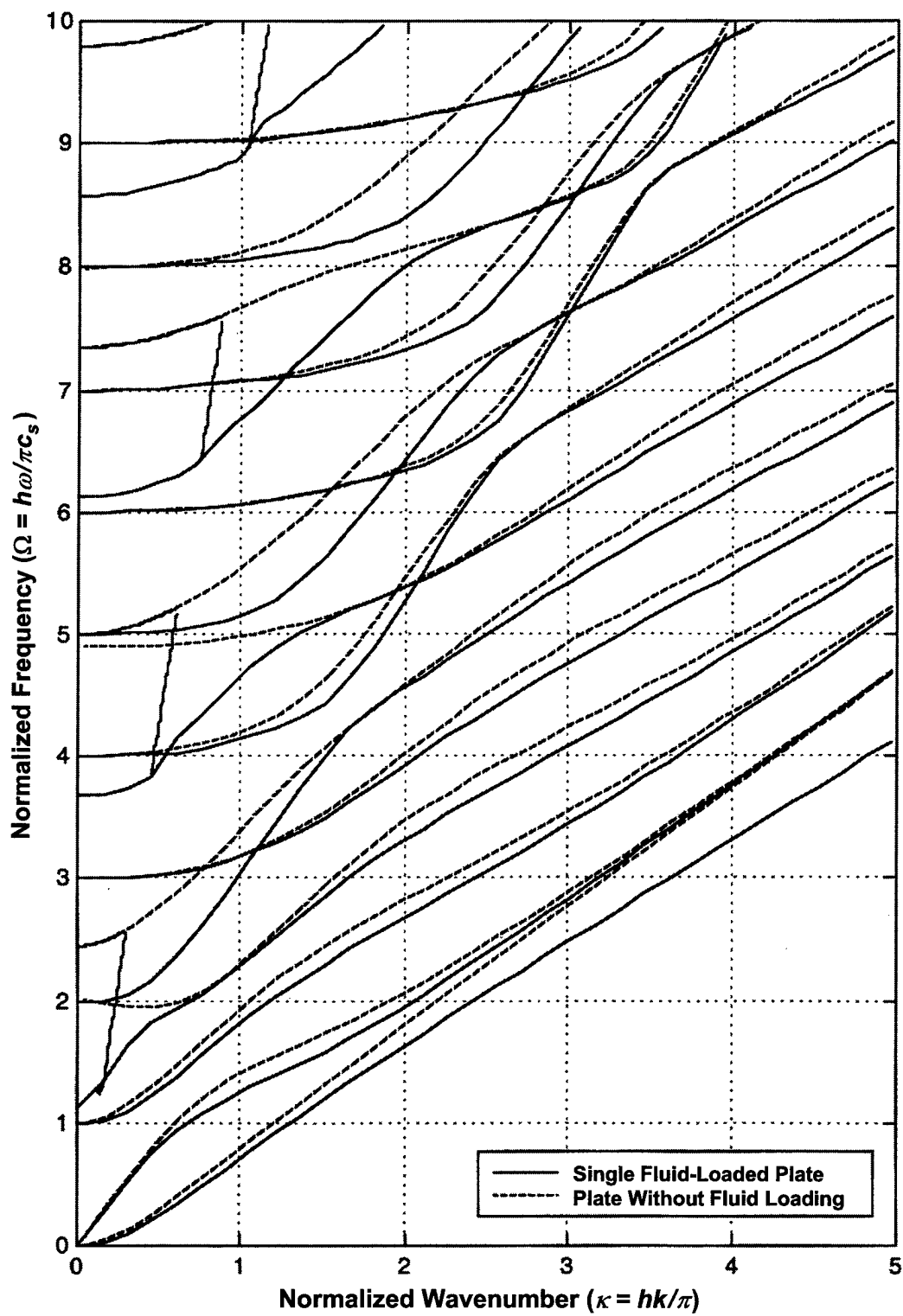
*Figure 4. Dispersion Curve for a Single Fluid-Loaded Plate
Compared to a Plate Without Fluid Loading*

21
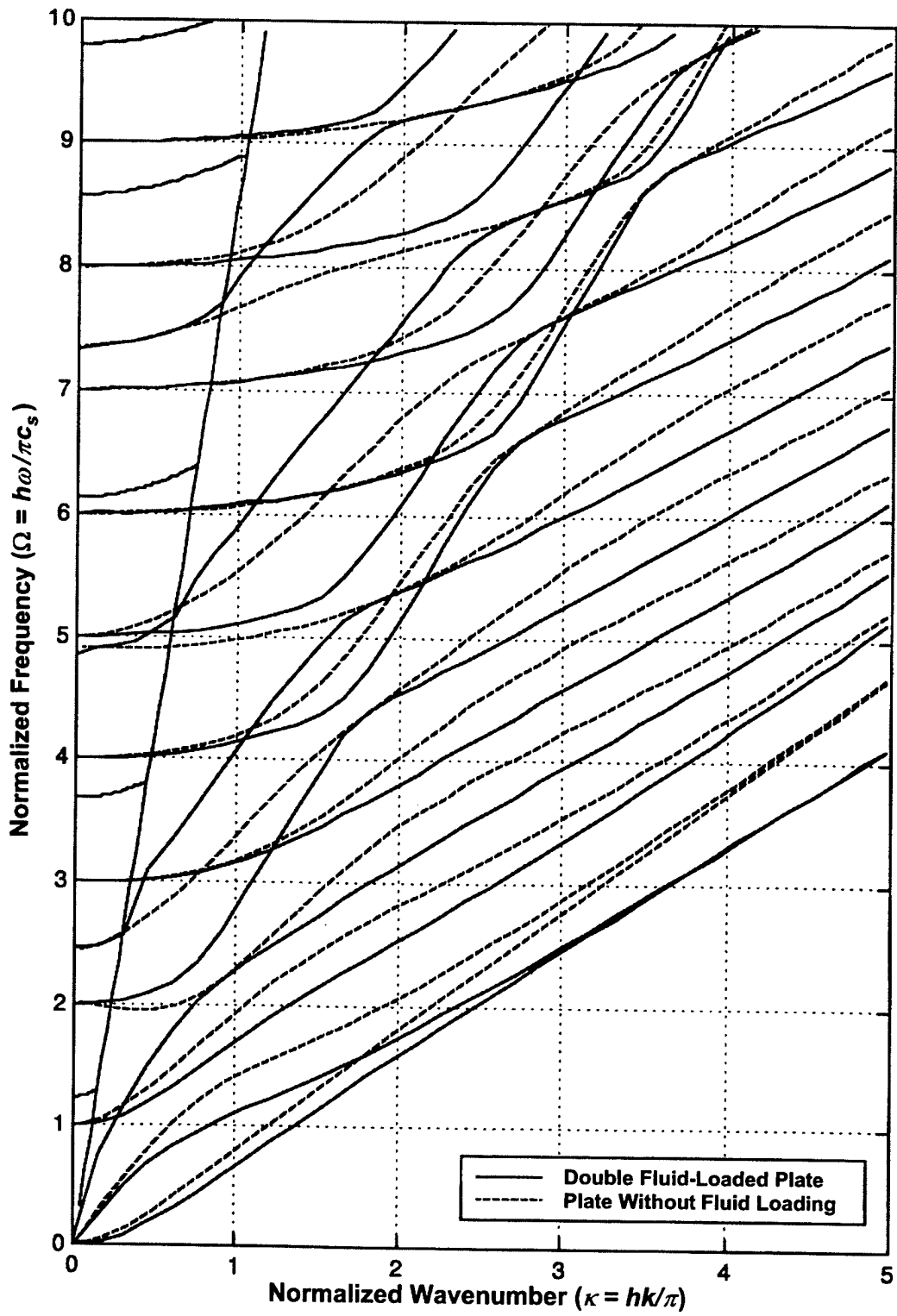
*Figure 5. Dispersion Curve for a Double Fluid-Loaded Plate
Compared to a Plate Without Fluid Loading*

22

medium. That is, at any given frequency, the maximum wavenumber of the energy traveling in the structure can be determined, which is advantageous for the analysis of turbulence-loaded structures where nonacoustic wave energy is present. Additionally, these curves can help in finite element models where proper mesh size is related to the wavenumber of energy propagation. Furthermore, these plots show the effects of fluid loading for each mode of propagation in the structure.

Figure 6 plots the transfer function of the tangential displacement divided by pressure versus normalized wavenumber with a normalized frequency of $\Omega = 5$ at location $z = -0.04$ m.[*] Figure 7 shows the transfer function of the normal displacement divided by pressure versus normalized wavenumber with a normalized frequency of $\Omega = 5$ at location $z = -0.04$ m. In both figures, the solid line represents the single fluid-loaded plate and the dashed line shows the plate without fluid loading.

Figure 8 plots the transfer function of the tangential displacement divided by pressure versus normalized wavenumber with a normalized frequency of $\Omega = 5$ at location $z = -0.04$ m. Figure 9 shows the transfer function of the normal displacement divided by pressure versus normalized wavenumber with a normalized frequency of $\Omega = 5$ at location $z = -0.04$ m. In these two figures, the solid line is the double fluid-loaded plate and the dashed line is the plate without fluid loading.

Figure 10 shows a displacement shape for the $n = 1$ antisymmetric mode of the double fluid-loaded plate, the single fluid-loaded plate, and the plate without fluid loading. The figure on the left illustrates plate thickness versus tangential displacement, and the figure on the right shows plate thickness versus normal displacement. The solid line is the double fluid-loaded plate, and the dashed line represents the single fluid-loaded plate and the plate without fluid loading. The displacement shapes were determined by taking a point on the $n = 1$ branch of each dispersion curve for the separate cases and then using these values to compute the displacements. For the double fluid-loaded plate, the values of this point were $\Omega = 2.94$ and $\kappa = 2.50$; for the single fluid-loaded plate, these values were $\Omega = 3.05$ and $\kappa = 2.50$; and for the plate without fluid loading, these values were $\Omega = 3.17$ and $\kappa = 2.50$. Note from equations (91), (97), (103), and (107) that the displacement shape is contained entirely in the numerator and that the location of

---

[*]In figures 6 through 9, the top plot is the magnitude and the bottom plot is the phase angle.
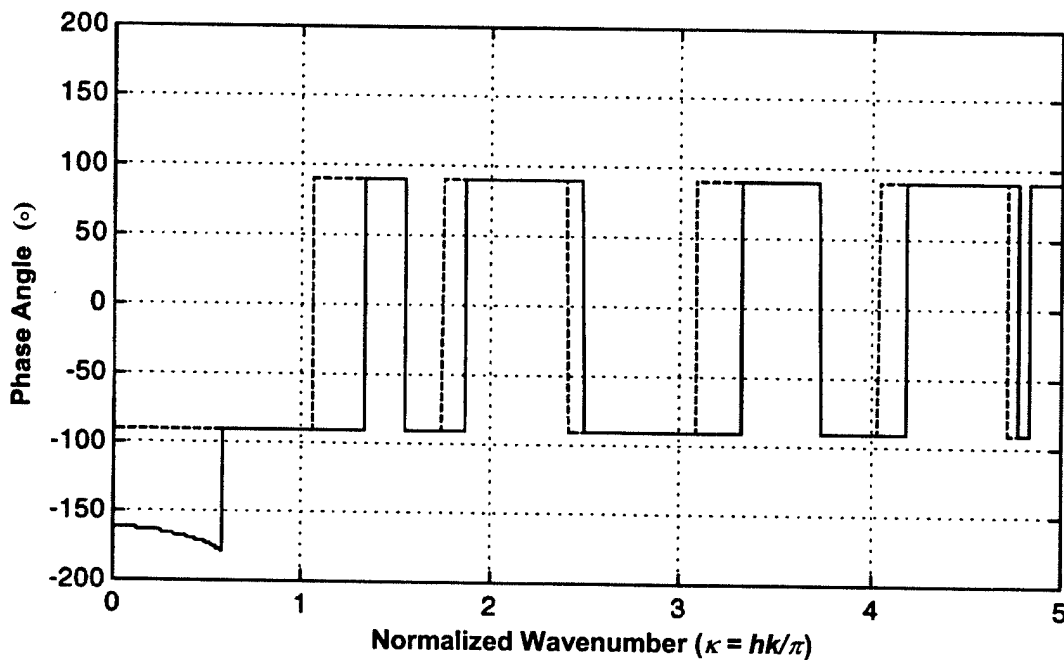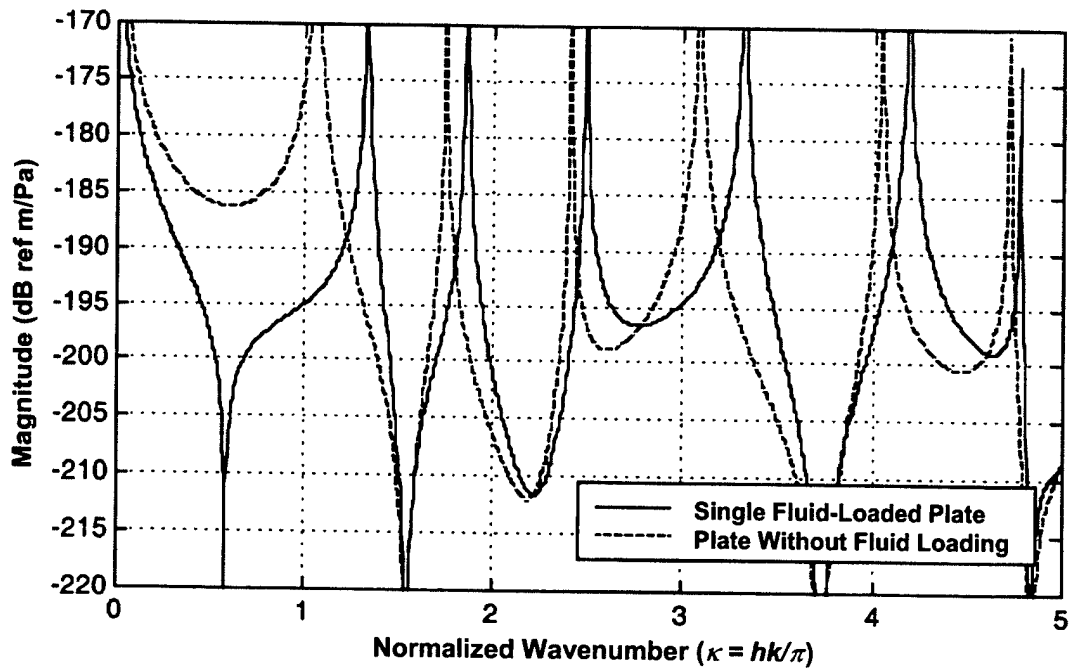
*Figure 6. Transfer Function of Tangential Displacement Divided by Pressure
Excitation Versus Normalized Wavenumber for a Single Fluid-Loaded Plate
Compared to a Plate Without Fluid Loading*
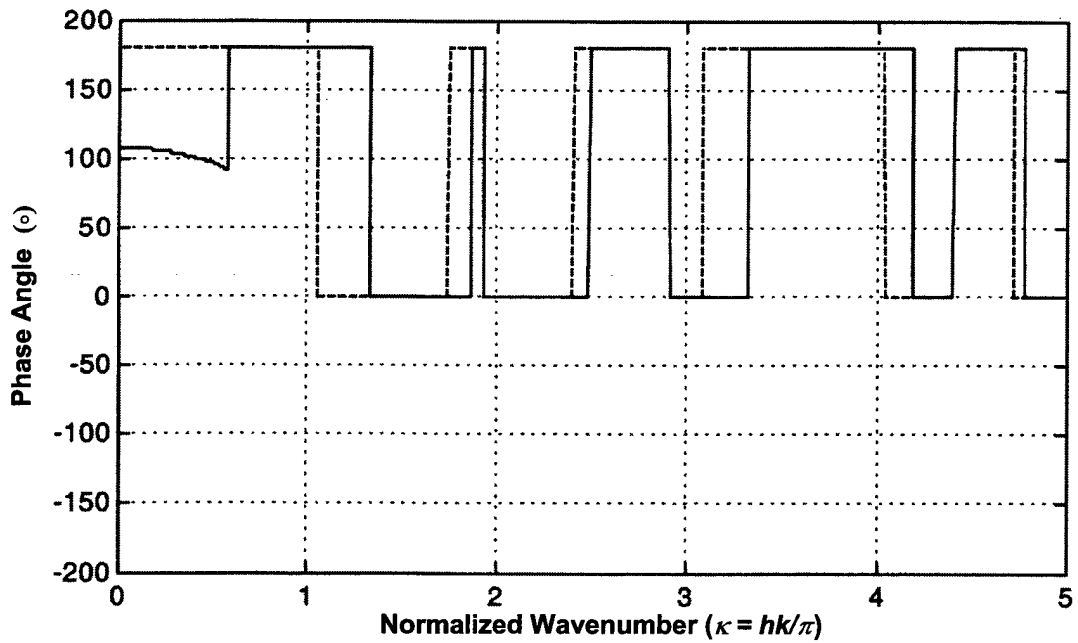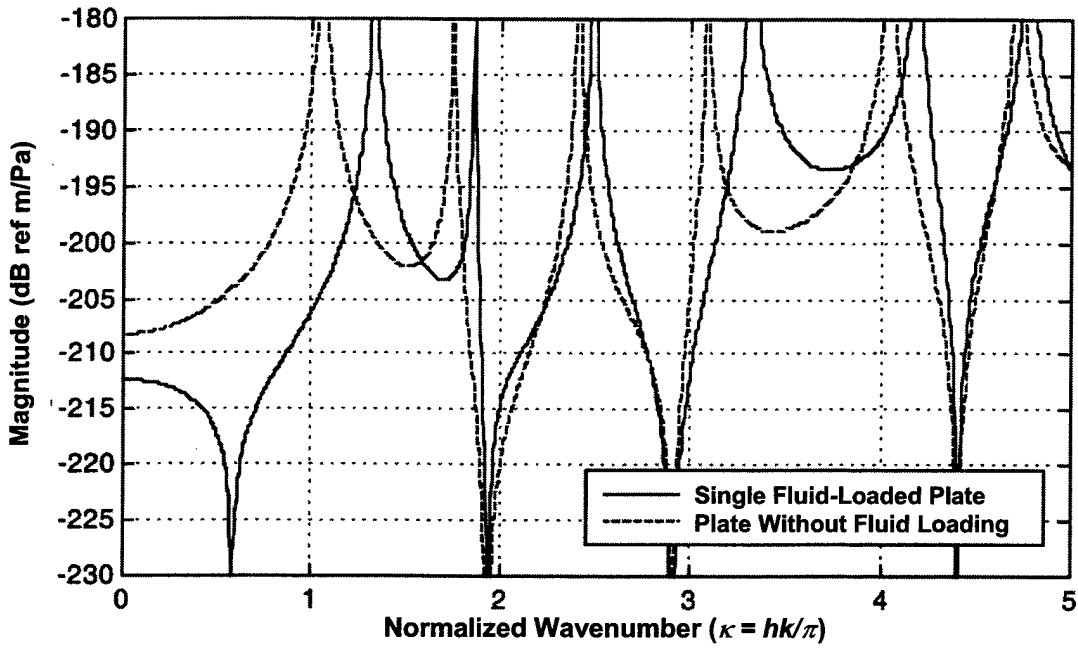
Figure 7. Transfer Function of Normal Displacement Divided by Pressure Excitation Versus Normalized Wavenumber for a Single Fluid-Loaded Plate Compared to a Plate Without Fluid Loading
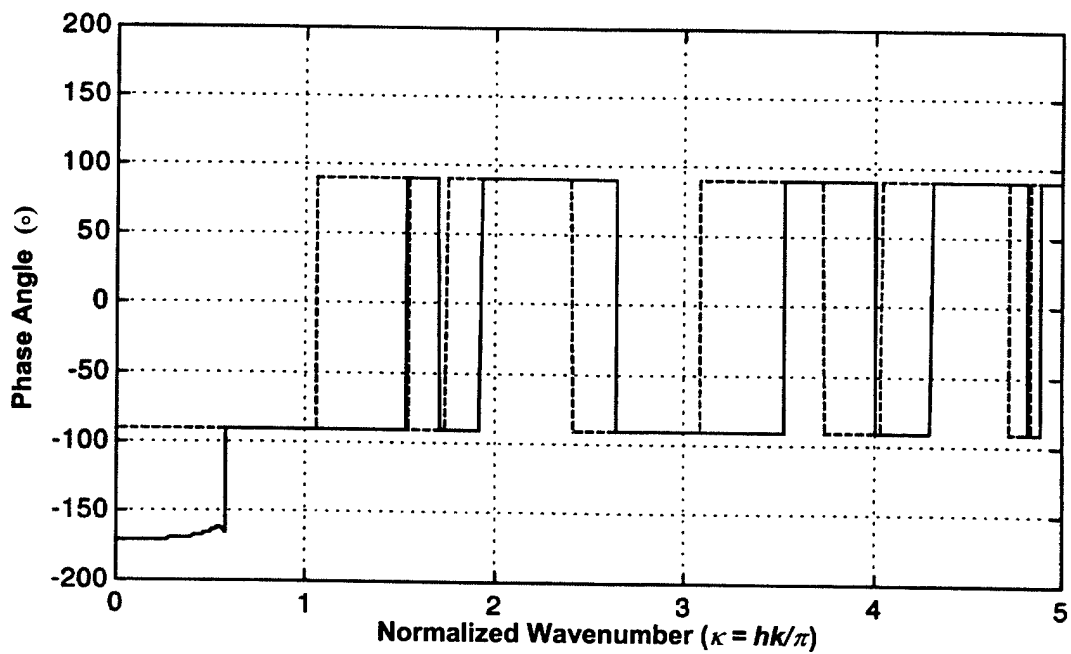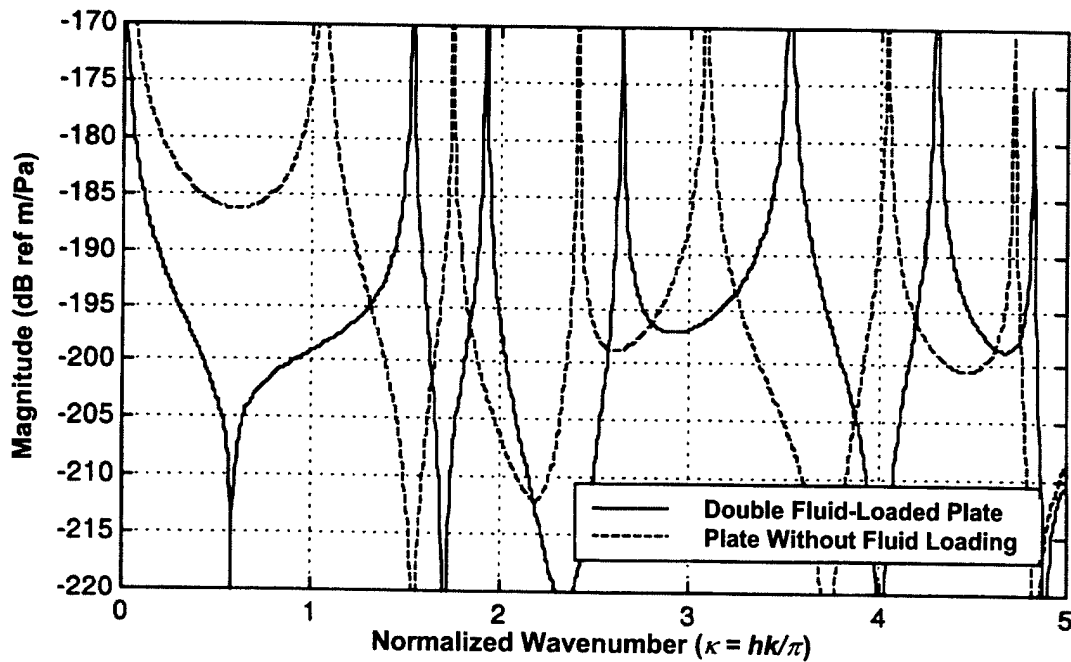
Figure 8. Transfer Function of Tangential Displacement Divided by Pressure Excitation Versus Normalized Wavenumber for a Double Fluid-Loaded Plate Compared to a Plate Without Fluid Loading
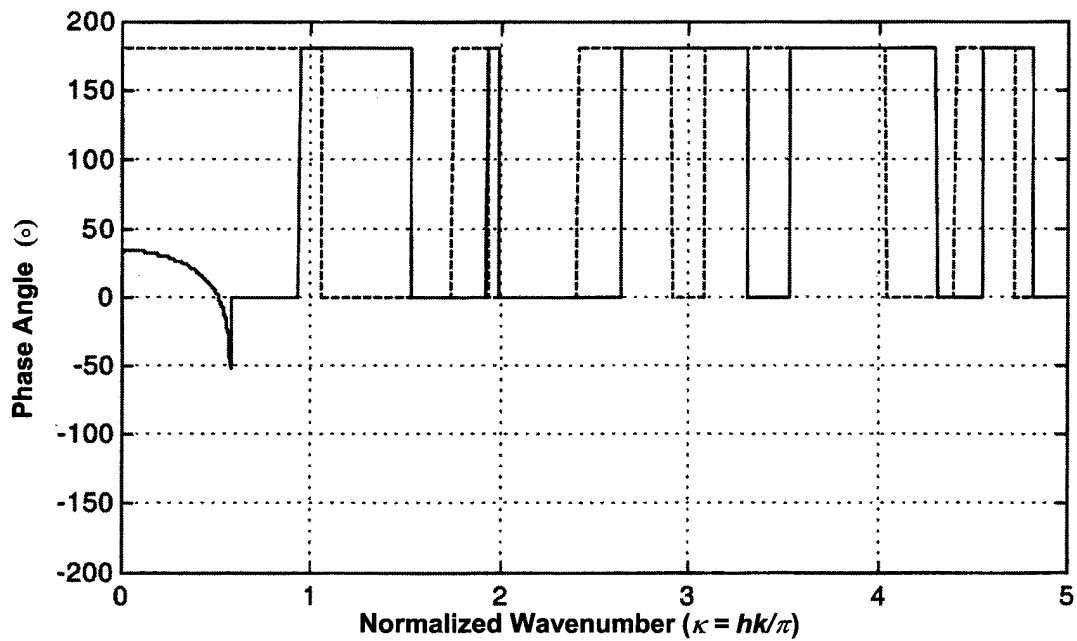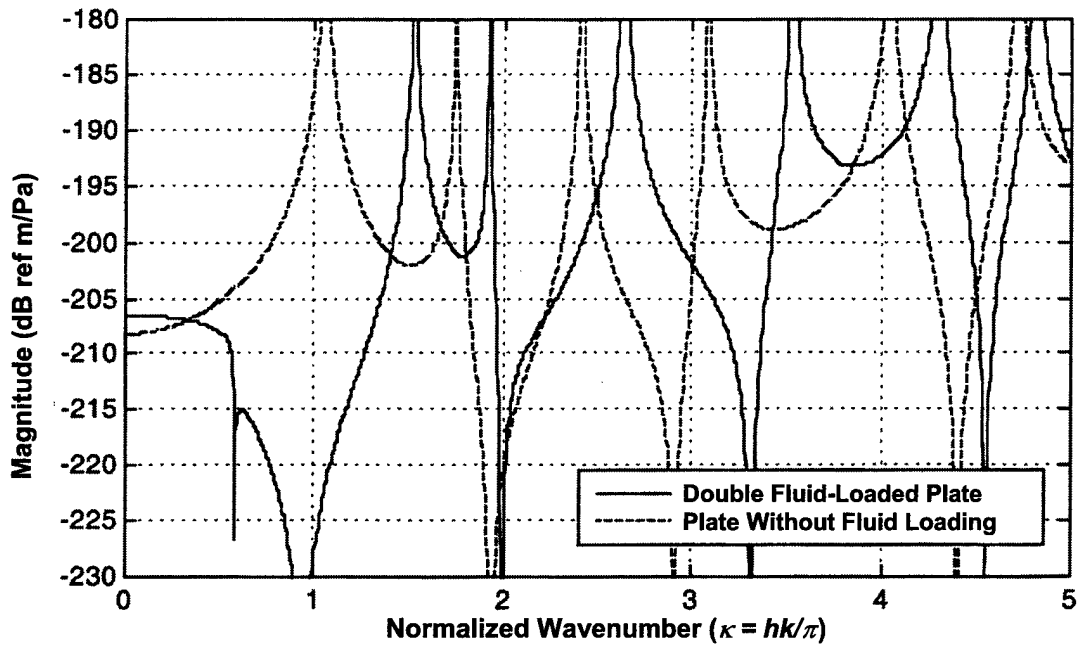
*Figure 9. Transfer Function of Normal Displacement Divided by Pressure
Excitation Versus Normalized Wavenumber for a Double Fluid-Loaded Plate
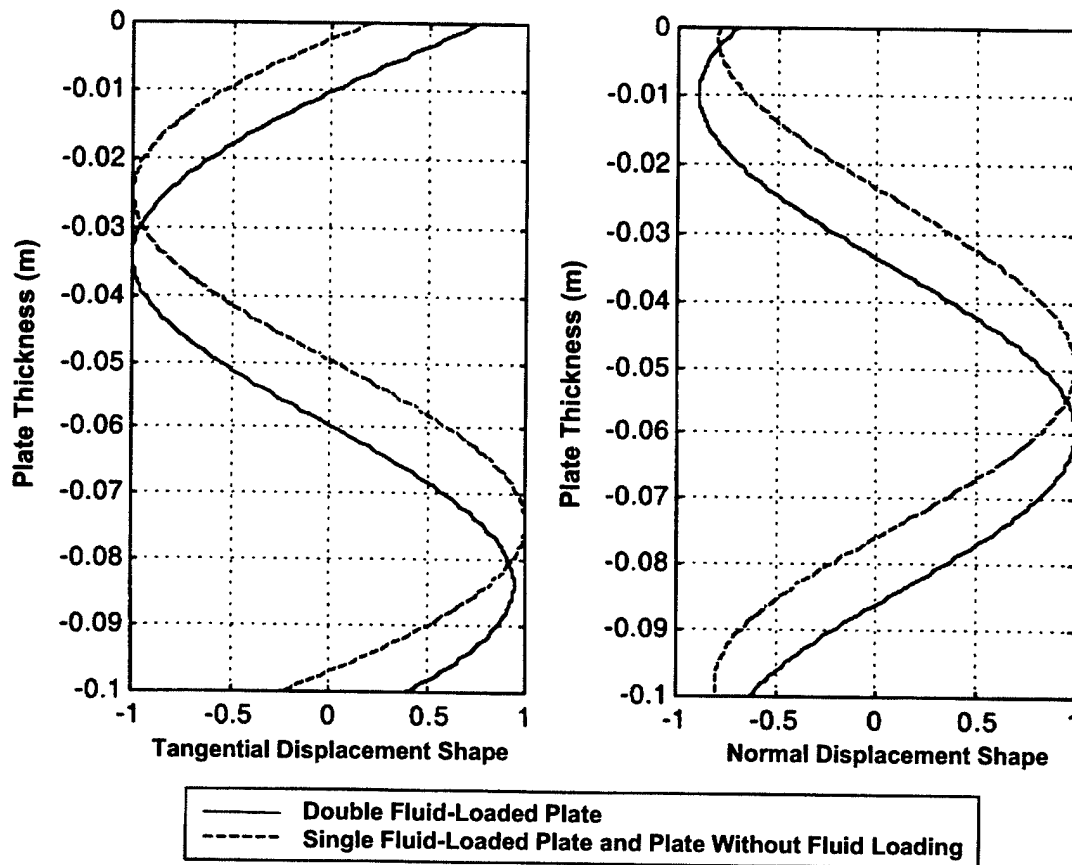Compared to a Plate Without Fluid Loading*

Figure 10. Displacement Shape of the n = 1 Mode for a Double Fluid-Loaded Plate Compared to a Single Fluid-Loaded Plate and a Plate Without Fluid Loading

the mode in the wavenumber-frequency plane is contained entirely in the denominator. Additionally, because the single fluid-loaded plate contains no fluid terms in the numerator, it has a displacement shape identical to the plate without the fluid load. However, the double fluid-loaded plate does contain fluid terms in the numerator, and thus its displacement shape is different from both the single fluid-loaded plate and the plate without fluid loading. Comparison of displacement shapes at other modes yields similar results to those of the unloaded, single-loaded, and double-loaded fluid plate displacement shapes shown in figure 10.

Figure 11 plots the magnitude of the insertion loss versus normalized frequency for the double fluid-loaded plate. The solid line corresponds to an acoustic wave at 45° incident to the plate, the dashed line corresponds to an acoustic wave at 0° incident to the plate (broadside), and the x's correspond to a closed-form solution given by[20]

$$IL(0,\omega) = 10\log_{10}\left|\left[\frac{(1-m^2)^2}{4m^2}\right]\sin^2(k_d h) + 1\right| ,$$

(119)

where

$$m = \frac{\rho c_d}{\rho_f c_f} .$$

(120)

Figure 12 shows the magnitude of the echo reduction versus normalized frequency for the double fluid-loaded plate. The solid line corresponds to an acoustic wave at 45° incident to the plate, the dashed line corresponds to an acoustic wave at 0° incident to the plate (broadside), and the x's correspond to a closed-form solution given by[20]

$$ER(0,\omega) = 10\log_{10}\left|\frac{4m^2}{[(1-m^2)^2 \sin^2(k_d h)]} + 1\right| .$$

(121)

It is noted that equations (119) and (121) are valid solely for excitation at zero wavenumber, where only dilatational wave motion is present. They do not account for nonzero wavenumbers, where the effects of shear wave motion is present. Also note in figures 11 and 12 that the shear wave energy originating at the integer normalized frequencies is present and creates a discontinuous function at the nonzero wavenumber, which is slightly (positively) shifted with respect to the frequency.
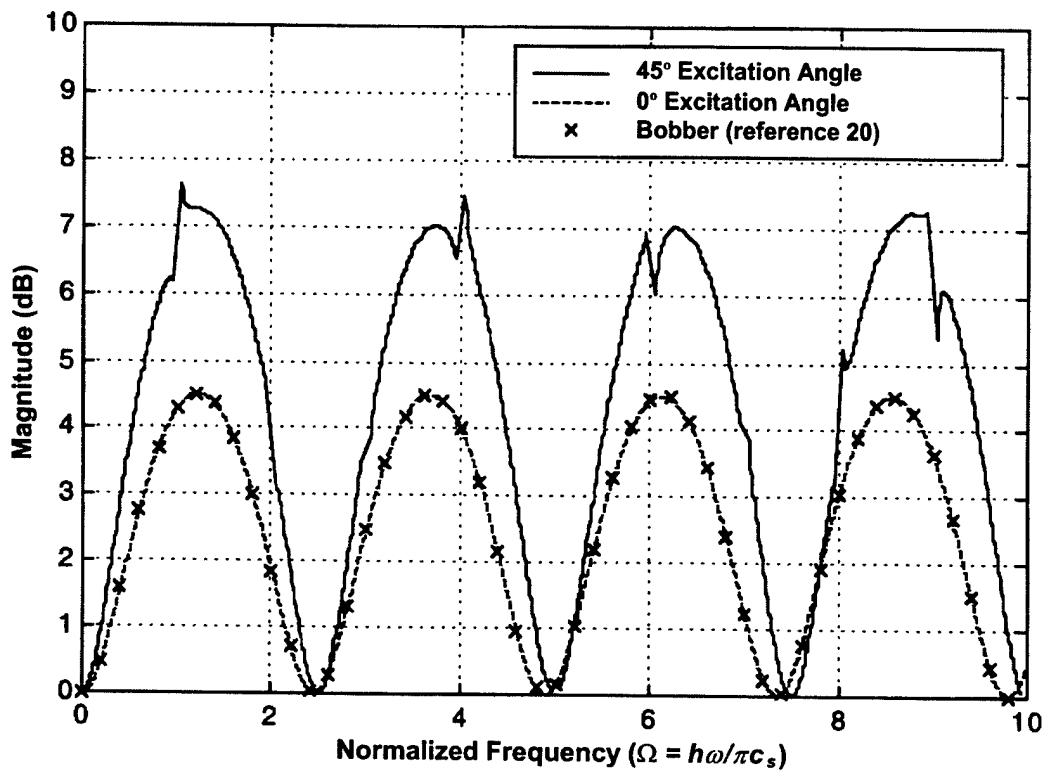
Figure 11. **Insertion Loss Versus Normalized Frequency**
for a Double Fluid-Loaded Plate
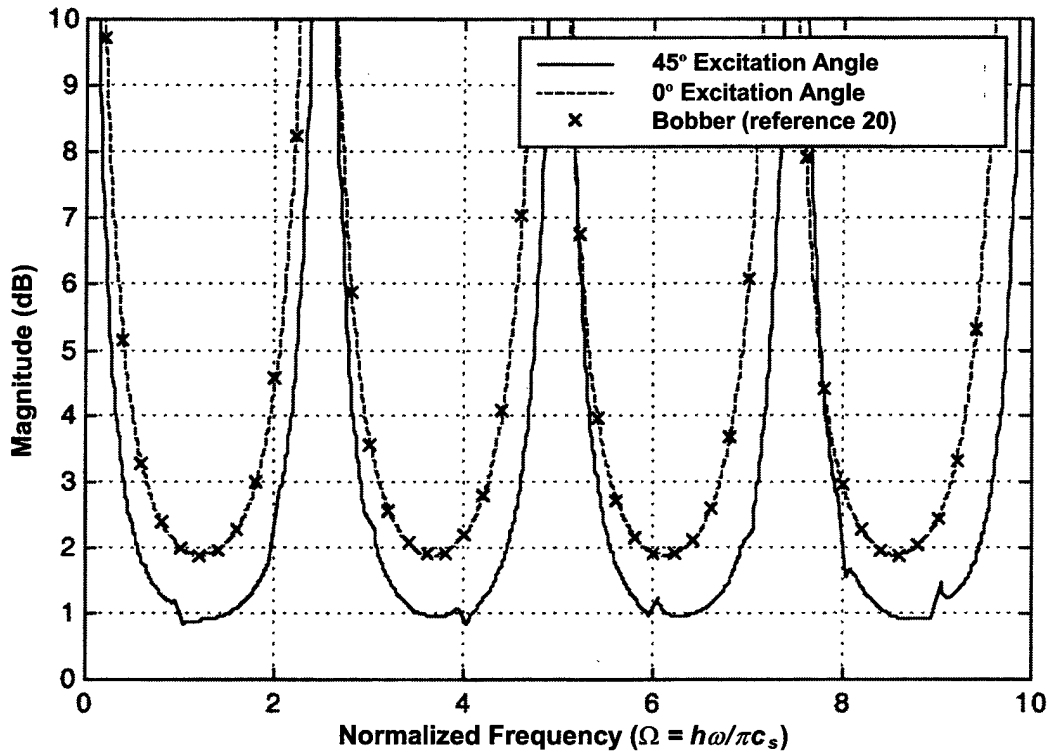
***Figure 12. Echo Reduction Versus Normalized Frequency
for a Double Fluid-Loaded Plate***

CONCLUSIONS AND RECOMMENDATIONS

This report has derived the closed-form solution to the expressions for insertion loss and echo reduction using a sample insonified at nonzero wavenumbers. Additionally, the closed-form transfer functions were derived for plate motion divided by excitation with fluid loading on one and both sides. The dispersion equation was also formulated based on the matrix equations and was then compared to previously available dispersion equation forms. It was shown that the zeros of both dispersion equations were in the same location. Furthermore, the displacement shapes of the system modes were determined, and it was found that the displacement shapes of the plate modes were identical for a plate with no fluid loading and for one with fluid loading on a single side. However, fluid loading on both sides produced a different displacement shape. Finally, closed-form transfer functions were derived that compared displacement across the plate rather than referenced to excitation levels. It was shown that plate dispersion curves were eliminated from the expressions that resulted when transfer functions were derived across the plate.

Future work in this area should investigate finite-sized plates, as well as anisotropic response.

REFERENCES

1. A. Leissa, *Vibration of Plates*, American Institute of Physics, College Park, MD, 1973.

2. H. Lamb, "On Waves in an Elastic Plate," *Proceedings of the Royal Society of London Series A*, vol. 93, 1917, pp. 114-120.

3. A. Freedman, "The Variation, with the Poisson Ratio, of Lamb Modes in a Free Plate, I: General Spectra," *Journal of Sound and Vibration*, vol. 137, no. 2, 1990, pp. 209-230.

4. A. Freedman, "The Variation, with the Poisson Ratio, of Lamb Modes in a Free Plate, II: At Transitions and Coincidence Values," *Journal of Sound and Vibration*, vol. 137, no. 2, 1990, pp. 231-247.

5. A. Freedman, "The Variation, with the Poisson Ratio, of Lamb Modes in a Free Plate, III: Behaviour of Individual Modes," *Journal of Sound and Vibration*, vol. 137, no. 2, 1990, pp. 249-266.

6. M. F. M. Osborne and S. D. Hart, "Transmission, Reflection, and Guiding of an Exponential Pulse by a Steel Plate in Water, I: Theory," *Journal of the Acoustical Society of America*, vol. 17, no. 1, 1945, pp. 1-18.

7. D. G. Crighton, "The Free and Forced Waves on a Fluid-Loaded Elastic Plate," *Journal of Sound and Vibration*, vol. 63, no. 2, 1979, pp. 225-235.

8. J. Dickey, G. Maidanik, and H. Überall, "The Splitting of Dispersion Curves for the Fluid-Loaded Plate," *Journal of the Acoustical Society of America*, vol. 98, no. 4, 1995, pp. 2365-2367.

9. A. Freedman, "Effects of Fluid Loading on Lamb Mode Spectra," *Journal of the Acoustical Society of America*, vol. 99, no. 6, 1996, pp. 3488-3496.

10. X. L. Bao, H. Franklin, P. K. Raju, and H. Überall, "The Splitting of Dispersion Curves for Plates Fluid Loaded on Both Sides," *Journal of the Acoustical Society of America*, vol. 102, no. 2, part 1, 1997, pp. 1246-1248.

11. K. Toda and K. Motegi, "Coupling of Velocity Dispersion Curves of Leaky Lamb Waves on a Fluid-Loaded Plate," *Journal of the Acoustical Society of America*, vol. 107, no. 2, 2000, pp. 1045-1048.

12. J. H. Su and R. Vasudevan, "On the Radiation Efficiency of Infinite Plates Subjected to a Point Load in Water," *Journal of Sound and Vibration*, vol. 208, no. 3, 1997, pp. 441-455.

13. W. A. Strawderman, *Wavevector-Frequency Analysis with Applications to Acoustics*, U.S. Government Printing Office, Washington, DC, 1996.

14. J. Wu and Z. Zhu, "The Propagation of Lamb Waves in a Plate Bordered with Layers of a Liquid," *Journal of the Acoustical Society of America*, vol. 91, no. 2, 1992, pp. 861-867.

15. P. M. Morse and K. U. Ingard, *Theoretical Acoustics*, Princeton University Press, Princeton, NJ, 1968.

16. S. P. Timoshenko and J. N. Goodier, *Theory of Elasticity*, McGraw-Hill Book Company, New York, 1934.

17. M. C. Junger and D. Feit, *Sound, Structures, and Their Interaction*, MIT Press, Cambridge, MA, 1986.

18. M. C. Potter, *Mathematical Methods in the Physical Sciences*, Prentice-Hall, Inc., Englewood Cliffs, NJ, 1978.

19. K. F. Graff, *Wave Motion in Elastic Solids*, Dover Publications, Inc., New York, 1975.

20. R. J. Bobber, *Underwater Electroacoustic Measurements*, Naval Research Laboratory, Washington, DC, July 1970.

APPENDIX

REDUCED-FORM TRANSFER FUNCTIONS OF DISPLACEMENT

Several reduced-form transfer functions of displacement at one side of the plate divided by displacement at the other side of the plate are presented in this appendix. These functions are especially useful when the data obtained during a test are accelerometer or laser velicometer data rather than fluid pressure data. Note that when the transfer function is formulated in this manner, the determinant is divided out of the equations. Moreover, the response of the plate without fluid loading is identical to the response of the single fluid-loaded plate.

The transfer function for the single fluid-loaded plate and the plate without fluid loading corresponding to the tangential displacement at $z = a$ divided by the tangential displacement at $z = b$ is

$$\frac{U_x(k_x, a, \omega)}{U_x(k_x, b, \omega)} = \frac{c_1[\cos(\alpha h) - \cos(\beta h)]}{\cos(\beta h)\cos(\alpha h) + c_2 \sin(\beta h)\sin(\alpha h) - 1}, \tag{A-1}$$

where

$$c_1(k_x, \omega) = \frac{\beta^2 + k_x^2}{\beta^2 - 3k_x^2} \tag{A-2}$$

and

$$c_2(k_x, \omega) = \frac{(\beta^2 - k_x^2)^3 - 8\alpha^2 \beta^2 k_x^2}{2\alpha\beta(\beta^2 - k_x^2)(\beta^2 - 3k_x^2)}. \tag{A-3}$$

The transfer function for the single fluid-loaded plate and the plate without fluid loading corresponding to the normal displacement at $z = a$ divided by the normal displacement at $z = b$ is

$$\frac{U_z(k_x, a, \omega)}{U_z(k_x, b, \omega)} = \frac{\sin(\alpha h) + c_3(k_x, \omega)\sin(\beta h)}{\sin(\alpha h)\cos(\beta h) + c_3(k_x, \omega)\cos(\alpha h)\sin(\beta h)}, \tag{A-4}$$

where

$$c_3(k_x, \omega) = \frac{(\beta^2 - k_x^2)^2}{4\alpha\beta k_x^2} \ . \tag{A-5}$$

The transfer function for the double fluid-loaded plate corresponding to the tangential displacement at $z = a$ divided by the tangential displacement at $z = b$ is

$$\frac{U_x(k_x, a, \omega)}{U_x(k_x, b, \omega)} = \frac{U_x^a(k_x, \omega)}{U_x^b(k_x, \omega)} \ , \tag{A-6}$$

where

$$\begin{aligned}
U_x^a(k_x, \omega) &= c_1(k_x, \omega)\cos(\alpha h) + d_1(k_x, \omega)\sin(\alpha h) \\
&\quad - c_1(k_x, \omega)\cos(\beta h) + d_2(k_x, \omega)\sin(\beta h) \ ,
\end{aligned} \tag{A-7}$$

$$\begin{aligned}
U_x^b(k_x, \omega) &= \cos(\alpha h)\cos(\beta h) + d_1(k_x, \omega)\sin(\alpha h)\cos(\beta h) \\
&\quad + d_2(k_x, \omega)\cos(\alpha h)\sin(\beta h) + c_2(k_x, \omega)\sin(\alpha h)\sin(\beta h) - 1 \ ,
\end{aligned} \tag{A-8}$$

$$d_1(k_x, \omega) = \frac{-i\rho_f \alpha(\beta^2 + k_x^2)^2}{\gamma\rho(\beta^2 - k_x^2)(\beta^2 - 3k_x^2)} \ , \tag{A-9}$$

and

$$d_2(k_x, \omega) = \frac{i\rho_f(\beta^2 + k_x^2)^2}{2\gamma\rho\beta(\beta^2 - 3k_x^2)} \ . \tag{A-10}$$

The transfer function for the double fluid-loaded plate corresponding to the normal displacement at $z = a$ divided by the normal displacement at $z = b$ is

$$\frac{U_z(k_x, a, \omega)}{U_z(k_x, b, \omega)} = \frac{U_z^a(k_x, \omega)}{U_z^b(k_x, \omega)} \ , \tag{A-11}$$

where

$$U_z^a(k_x, \omega) = c_3(k_x, \omega)\sin(\beta h) + \sin(\alpha h) \ , \tag{A-12}$$

$$U_z^b(k_x,\omega) = c_3(k_x,\omega)\cos(\alpha h)\sin(\beta h) - d_3(k_x,\omega)\sin(\alpha h)\sin(\beta h)$$
$$+ \sin(\alpha h)\cos(\beta h)\,, \tag{A-13}$$

and

$$d_3(k_x,\omega) = \frac{i\rho_f(\beta^2 + k_x^2)^2}{4\gamma\rho\beta k_x^2}\,. \tag{A-14}$$

INITIAL DISTRIBUTION LIST

Addressee	No. of Copies
Office of Naval Intelligence (ONI 241 – J. Zilius, T. Morgan; ONI 263 – S. Brown (2))	4
Office of Naval Research (ONR 321 – R. Elswick; ONR 333 – K. Ng)	2
Defense Technical Information Center	2
Center for Naval Analyses	1